Utilising graphene antidots for implementation of a broadband terahertz absorber

Kamal Jamalpoor, Abbas Zarifkar ✉

School of Electrical and Computer Engineering, Shiraz University, Shiraz, Fars, Iran
✉ *E-mail: zarifkar@shirazu.ac.ir*

Published in Micro & Nano Letters; Received on 23rd April 2018; Revised on 15th July 2018; Accepted on 28th August 2018

In this work, a broadband absorber is designed for application in the terahertz region using graphene antidots array. The proposed absorber consists of an Au substrate, a polyethylene dielectric layer and a graphene sheet with antidot resonators. The geometrical dimensions of the antidot resonator and its array period, the graphene conductivity parameters and the dielectric layer height and refractive index are the parameters that determine the characteristics of the absorber such as bandwidth, centre frequency, the amount of the absorption and sensitivity to the incident wave incident angle and polarisation. The circuit theory and a broadband matching technique of the transmission lines are utilised in some steps of the design approach. Moreover, some rules of thumb are extracted for the absorber design in different frequencies. The designed absorber has a normalised bandwidth of 80% in the terahertz region, low sensitivity to incident angle and an absorption peak of 100%.

1. Introduction: The electromagnetic field absorption has been the centre of attention in the design of devices such as wavelength-tunable microbolometers [1], thin-film solar cells [2], electromagnetic absorbers based on plasmonics and metamaterial [3] and so on. Among many absorbing materials, graphene, a two-dimensional material with honeycomb formation, seems to be a suitable candidate because of its capability of absorption based on surface plasmon polaritons (SPPs) at THz frequencies [4–7]. In addition, quantum Hall effect [8], gate-variable optical conductivity [9] and controllable plasmonic properties [10] are some of the exceptional electrical and optical properties of graphene. The graphene-based absorbers can be tunable [4] and broadband (in THz regime) [5] which are important properties in some applications.

It is reported in [11] that the terahertz electromagnetic wave transmission through a stack of monolayer graphene sheets (without patterning) can be tuned with bias voltage. Also, it is shown that layers of graphene patches separated by dielectric slabs construct a tunable absorber that absorbs energies in the intervals with narrow frequency band [12].

Periodic patterns increase the coupling of the incident wave to the SPPs and consequently improve the overall absorption. Absorber designs based on periodic arrays of graphene nano-disks [7, 13] and nano-ribbons [14] have been shown to fully absorb electromagnetic waves within the terahertz region.

The bandwidth of metal-based plasmonic absorbers has been reported to be narrow in the terahertz region [15–17] that originates from the narrow bandwidth of SPPs generated on metallic surfaces [5]. However, recently, the graphene-based absorbers have been reported to have broader bandwidth. The recent approaches to meet the broad bandwidth and almost total absorption in graphene-based absorbers include: several patterned graphene layers stacked on top of each other and biased at different voltages [5], periodic array of graphene ribbons fabricated at an appropriate distance from a metallic ground plate [6, 14], arrays of doped graphene nano- and micro-disks supported by a substrate for total internal reflection and a dielectric layer [7, 13] and periodically patterned cross-shaped graphene arrays [18].

Interestingly, the incidence angle and polarisation dependence of the graphene absorbers are caused by the symmetry of the graphene resonator so that in the case of disk or cross-shaped resonator, the absorber is polarisation independent [13, 18]. On the other hand, the ribbon resonators lead to absorption of only transverse magnetic (TM) polarised incident waves [14].

In all the abovementioned designs of the graphene-based absorbers, graphene is needed to be biased so that the device can be applicable in the terahertz regime and the advantage of the device tunability emerges. However, from the experimental point of view, it is very hard to apply equal bias voltages to an array of resonators. In addition, in the electronic devices that use such an absorption mechanism for the wave detection, there must be a path for the excited current to reach the bias contacts [18].

In the present work, a novel structure of graphene-based absorber is presented. It consists of an array of graphene antidots that are placed on a dielectric layer coating a metal. The absorber has a broad bandwidth and is insensitive to polarisation and incident angle variations. Moreover, it does not need many biasing circuits and only one bias position is enough. Similar to [13, 14], the circuit theory is utilised in the design procedure.

This Letter includes the following sections. In Section 2, a transmission line broadband matching technique is used for achieving the graphene conductivity parameters. In Section 3, the dimension of the antidot resonators and the array period are obtained and the absorber sensitivity to some dimensions variation is investigated. In the final section, conclusion is presented.

2. Absorber design using circuit model: The absorber structure, as shown in Fig. 1, includes a graphene sheet with an array of antidot resonators with the radius of a and array period of L, a polyethylene layer with the height and refractive index of d and n_s, respectively, and a thick Au layer with finite conductivity. In addition, it is supposed that the incident wave with the electric field along the x-axis is normal to the graphene surface.

The graphene surface conductivity is derived using the Kubo formula [19]

$$\sigma_s = \frac{2e^2 k_B T}{\pi h^2}\frac{j}{j\tau^{-1}-\omega}\ln\left[2\cosh\left(E_F/2k_B T\right)\right] - \frac{je^2}{4\pi h}\ln\left[\frac{2E_F - h(\omega - j\tau^{-1})}{2E_F + h(\omega - j\tau^{-1})}\right] \quad (1)$$

where e, k_B, $\hbar$, T, E_F, ω and τ are the electron charge, the Boltzmann constant, the Plank constant, the temperature (300 K), the Fermi energy, the angular frequency and the relaxation time, respectively.

Actually, the goal is to find the suitable parameters for the graphene conductivity, the dielectric layer refractive index and the geometrical dimensions of the resonators to meet the broadband absorption.

doi: 10.1049/mnl.2018.5079

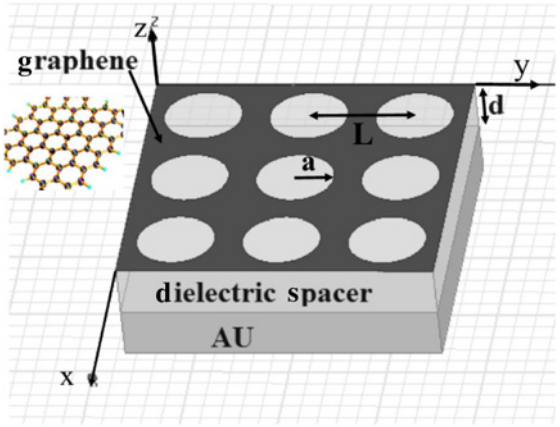

Fig. 1 *Proposed structure for the broadband and polarisation insensitive absorber. It consists of a graphene sheet with an array of antidots on top of a dielectric layer spacer and Au substrate*

Since the equivalent circle model of the antidot graphene resonators array has not been investigated so far, the procedure of absorber design using circuit model [13, 14] is only applicable in some steps.

Suppose that the equivalent circuit of the proposed absorber is as shown in Fig. 2, where the free space and the dielectric layer are modelled as transmission lines with the admittances of Y_0 and Y_s, respectively, and Y_{Au} is the admittance of Au layer. R_1, L_1 and C_1 represent the equivalent circuit model of the antidot resonators that are unknown in this Letter. The indexes show that the equivalent circuit of array resonators would contain many parallel RLCs and here we may only use the dominant resonance for simplicity.

Since the absorber is designed for the terahertz region, Au acts like a perfect electric conductor (PEC). Consequently, the abovementioned admittances values are as follows: $Y_0 = \eta_0^{-1}$, $Y_s = n_s\eta_0^{-1}$ and $Y_{\text{Au}} \simeq \infty$ where $\eta_0 = 376.73\,\Omega$ is the free space intrinsic impedance.

Obviously, $Y_{in1} = Y_{in2} + Y_{\text{g}}$ where Y_{g} is the admittance of the graphene antidot array that is shown by a series of R_1, L_1 and C_1. By choosing $d = \lambda/4$ or $\beta_s d = \pi/2$, where β_s is the propagation constant of the dielectric layer, the dielectric layer acts like a $\lambda/4$ transformer, i.e. $Y_{in2} = 0$, where λ is the free space wavelength and c is the light speed in vacuum.

$$\beta_s = \frac{2\pi n_s f_0}{c} \tag{2}$$

$$d = \frac{c}{4n_s f_0} \tag{3}$$

$$Y_{in2} = Y_s \frac{Y_{\text{Au}} + jY_s \tan\beta_s d}{Y_s + jY_{\text{Au}} \tan\beta_s d} \tag{4}$$

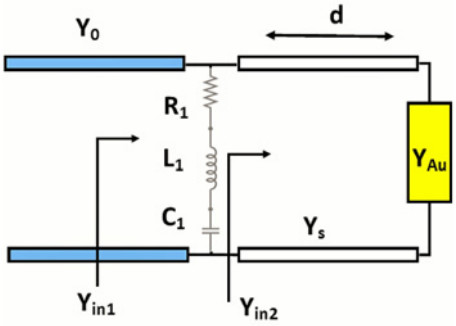

Fig. 2 *Equivalent circuit of the antidot graphene absorber*

Consequently, the input admittance of the absorber gets equal to the graphene admittance, i.e. $Y_{in1} = Y_{\text{g}}$

$$Y_{\text{g}} = \frac{1}{R_1 + j\omega L_1 + (j\omega C_1)^{-1}} \tag{5}$$

In order to meet the matching condition, the following relations must be satisfied:

$$R_1 = \eta_0 \tag{6}$$

$$f_0 = \frac{1}{2\pi\sqrt{L_1 C_1}} \tag{7}$$

However, the above relations lead to narrow-band absorption. Therefore, the following conditions will be applied in order to meet the broadband matching:

$$\text{Re}(Y_{in1}) = R_1^{-1} = \gamma/\eta_0 \tag{8}$$

$$\frac{\text{d}}{\text{d}f}\text{Im}(Y_{in1}) = 0 \tag{9}$$

where γ is a coefficient larger than unity. The two last relations lead to an increase in the bandwidth but may decrease the perfect matching or absorption. However, we try to meet the most possible absorption which means the least return loss, Γ. Supposing $\Gamma^2 < 0.1$, we have

$$\left(\frac{Y_0 - Y_L}{Y_0 + Y_L}\right)^2 < 0.1$$
$$\left(\frac{1-\gamma}{1+\gamma}\right)^2 < 0.1 \tag{10}$$

So, $\gamma < 1.925$ and is assumed to be 1.9.

It can be concluded from the relation between R_1 and L_1 in [13, 14] that regardless of the resonator geometry, $L_1 = \tau R_1$. Moreover, it is proved that when the working frequency is around the centre frequency f_0, by combining (3) and (4), the relaxation time τ for the graphene-based resonator is calculated as follows, regardless of the resonators shape [13, 14]

$$\tau = \frac{n_s}{8\beta\gamma f_0} \tag{11}$$

where β is the scaling factor and initially it is set to 1. Providing that n_s and f_0 are set to 1.5 and 1 THz, respectively, the relaxation time, τ, and the dielectric layer height, d, are calculated to be 9.8684×10^{-14} and 50 μm, respectively. Since $\tau = \mu E_{\text{F}}/e\nu_{\text{F}}^2$ [20], the Fermi energy is calculated as 0.493 eV, where $\mu = 0.2\,\text{m}^2/\text{Vs}$ and $\nu_{\text{F}} = 10^6\,\text{m/s}$ are the electron mobility and the Fermi velocity, respectively.

At this step of the absorber design, all of the unknown parameters including the graphene conductivity parameters, the dielectric layer dimensions and refractive index are calculated except for the parameters that belong to the resonator shape and the array period.

Unfortunately, the equivalent circuit of the graphene antidot resonators is not available, so, the two left structure parameters a and L and consequently the equivalent circuit parameters R_1, L_1 and C_1 cannot be calculated. Therefore, a and L are extracted using the full-wave simulation in HFSS software. In other words, one may design an identical absorber with any optional resonator shape, providing that the parameters which are related to the resonators shape and the array period get extracted through the full-wave simulations.

3. Simulations: There are two ways to simulate array of resonators in HFSS. The first is using floquet ports and master–slave periodic boundary condition pairs, and the second is to use PEC and perfect magnetic conductor boundary conditions. The analysis in the latter approach is converged faster and has a more precise output.

Although the thickness of the graphene sheet is 0.34 nm in reality, the simulations show that the results do not change when the graphene thickness is varied from 0.34 to 1 nm [21], consequently, the graphene thickness is chosen 1 nm in the current work. In addition, the Au substrate is defined as a PEC sheet. Therefore, the graphene relative permittivity is required that is calculated by [22]

$$\varepsilon_{\rm gr} = 2.5 + i\frac{\sigma_s}{\omega\varepsilon_0\Delta} \tag{12}$$

where $\Delta = 1$ nm is the graphene thickness. After some optimisations, the suitable values of a and L for the perfect absorption in the normalised bandwidth of 80% are achieved that is shown in Fig. 3. The effects of the antidots diameter and period changes are shown in Figs. 4 and 5, respectively.

As expected, the following points can be concluded from the simulations:

(i) a and L are proportional to the inverse of f_0. Comparing this point with the results of [13, 14], it is more precise to say that a and L are proportional to $1/f_0^2$.

(ii) The decrease of a or increase of L leads to increase in the area of the resonator and therefore in the amount of absorption.

(iii) For a constant value of a/L ratio, the amount of the absorption and its centre frequency remain partly unchanged although a and L may vary.

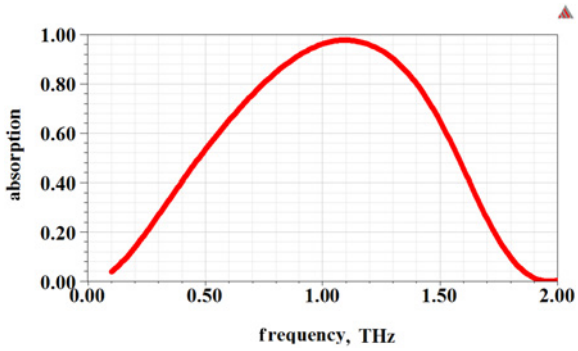

Fig. 3 *Simulated absorption of the graphene antidot absorber with the parameters a = 40 μm and L = 110 μm*

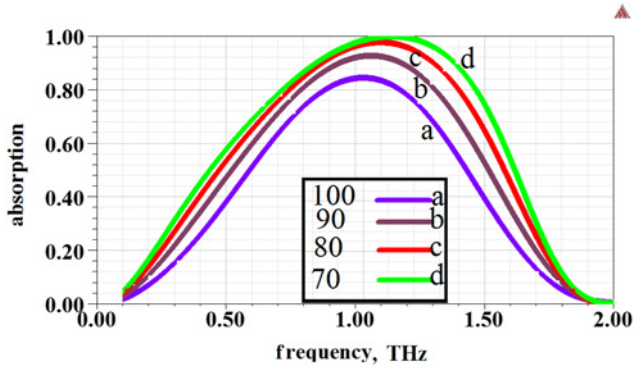

Fig. 4 *Simulated absorption for different values of the antidots diameter, 2a, in μm*

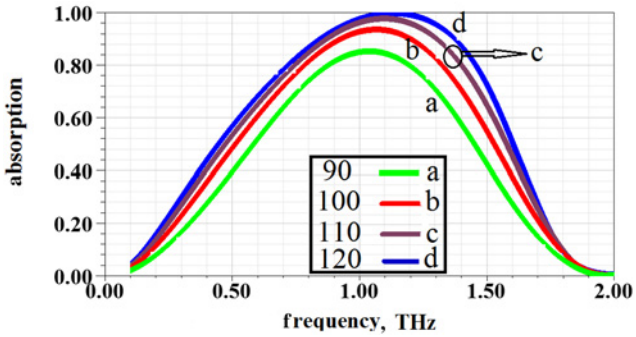

Fig. 5 *Simulated absorption for different values of the array period, L, in μm*

The optimised value for the ratio of a/L is almost 36%. In order to check the validity of this result, another absorber with the centre frequency of 0.5 THz is designed below.

We set the scaling factor β equal to 2, therefore, for the centre frequency of 0.5 THz, τ and $E_{\rm F}$ are the same as before from (11), while from (3), $d = 100$ μm. Since a and L are proportional to $1/f_0^2$, they are multiplied by 4, so, their values are $a = 160$ μm and $L = 440$ μm. Fig. 6 shows the absorption spectrum for the simulated structure with the exact centre frequency of 0.5 THz and normalised bandwidth of near 85%.

Since the resonator shape is symmetric in the x–y plain, the proposed absorber is expected to be polarisation insensitive for the normal incident beams. As shown in Fig. 7 for tilt angles of incident wave with transverse electric (TE, red line) and TM (blue line) polarisations and different incident angles (almost 60°), the absorption would not change substantially.

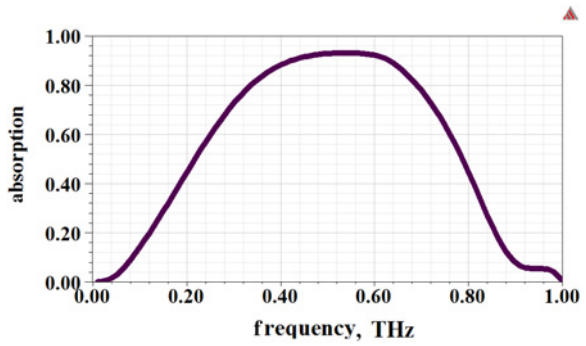

Fig. 6 *Absorption spectrum for the absorber with the centre frequency of 0.5 THz*

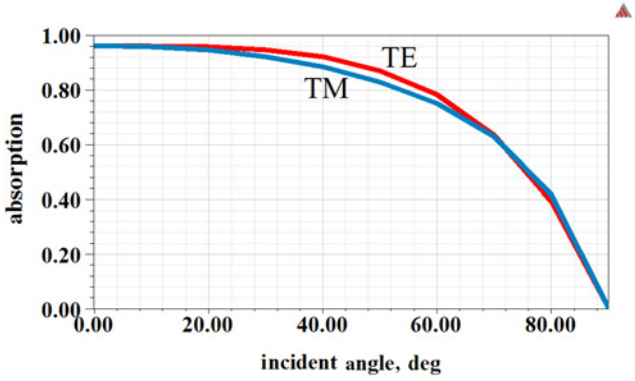

Fig. 7 *Absorption versus incident angle for two incident wave polarisations (TE in red and TM in blue)*

doi: 10.1049/mnl.2018.5079

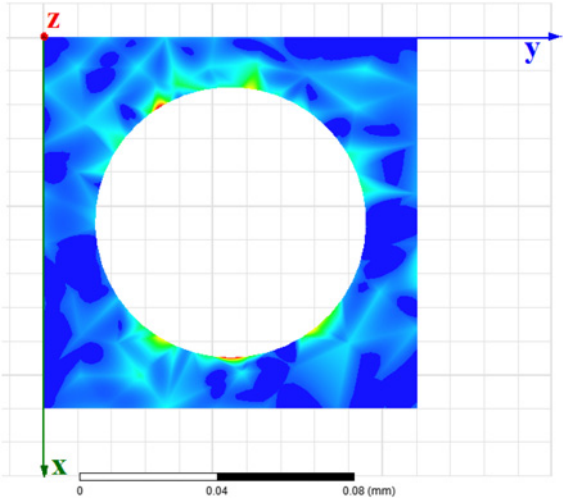

Fig. 8 *Excited current on the graphene antidot absorber*

The incident waves can excite current on graphene resonator array providing that some conditions get satisfied [7, 22]. The induced current distribution on a graphene disk and ribbon are extracted in [23, 24], respectively. The main advantage of the proposed absorber to the other similar structures is that the excited current can be collected via the contact through which the bias voltage is applied. The excited current profile on the graphene surface is shown in Fig. 8. This current is desirable in the devices such as sensors or detectors.

4 Conclusion: In this Letter, a broadband terahertz absorber is designed that is insensitive to the polarisation and uses a graphene sheet with antidot resonators as a main absorbing material. The design parameters related to the surface conductivity of graphene and the dielectric layer refractive index and its dimensions are extracted using circuit theory. Moreover, the parameters corresponding to the resonator shape and array period are obtained using full-wave simulations. The circuit theory helps to design a broadband matching section and the resonator shape specifies the sensitivity to polarisation change. Finally, some rules of thumbs are extracted so that one may design the absorber for other terahertz frequencies, too. The absorber shows normalised bandwidth of 80% and the peak absorption of 100% while it needs only one bias contact for all array resonators. In addition, polarisation change (TE and TM) and incident angle variation (up to 60°) do not have significant impacts on the amount of absorption.

5 References

[1] Maier T., Brückl H.: 'Wavelength-tunable microbolometers with metamaterial absorbers', *Opt. Lett.*, 2009, **39**, pp. 3012–3014

[2] Pala R.A., White J., Barnard E., *ET AL.*: 'Design of plasmonic thin-film solar cells with broadband absorption enhancements', *Adv. Mater*, 2009, **21**, pp. 3504–3509

[3] Cui Y., He Y., Jin Y., *ET AL.*: 'Plasmonic and metamaterial structures as electromagnetic absorbers', *Laser Photonics Rev.*, 2014, **8**, pp. 495–520

[4] Xu B., Gu Ch., Li Zh., *ET AL.*: 'A novel structure for tunable terahertz absorber based on graphene', *Opt. Express*, 2013, **21**, pp. 23803–23811

[5] Amin M., Farhat M., Bağcı H.: 'An ultra-broadband multilayered graphene absorber', *Opt. Express*, 2013, **21**, pp. 29938–29948

[6] Alaee R., Farhat M., Rockstuhl C., *ET AL.*: 'A perfect absorber made of a graphene micro-ribbon metamaterial', *Opt. Express*, 2012, **20**, pp. 28017–28024

[7] Thongrattanasiri S., Koppens F.H.L., García de Abajo F.J.: 'Complete optical absorption in periodically patterned graphene', *Phys. Rev. Lett.*, 2012, **108**, p. 047401

[8] Andryieuski A., Lavrinenko A.: 'Graphene metamaterials based tunable terahertz absorber: effective surface conductivity approach', *Opt. Express*, 2013, **21**, pp. 9144–9155

[9] Wang F., Zhang Y., Tian Ch., *ET AL.*: 'Gate-variable optical transitions in graphene', *Science*, 2008, **320**, pp. 206–209

[10] Xia F., Mueller T., Lin Y., *ET AL.*: 'Ultrafast graphene photodetector', *Nat. Nanotechnol.*, 2009, **4**, pp. 839–843

[11] Kaipa Ch.S.R., Yakovlev A.B., Hanson G.W., *ET AL.*: 'Enhanced transmission with a graphene-dielectric microstructure at low-terahertz frequencies', *Phys. Rev. B*, 2012, **85**, p. 245407

[12] Fallahi A., Perruisseau-Carrier J.: 'Design of tunable biperiodic graphene metasurfaces', *Phys. Rev. B*, 2012, **86**, p. 195408

[13] Arik K., Ramezani S.A., Khavasi A.: 'Polarization insensitive and broadband terahertz absorber using graphene disks', *Plasmonics.*, 2017, **12**, pp. 393–398

[14] Khavasi A.: 'Design of ultra-broadband graphene absorber using circuit theory', *J. Opt. Soc. Am. B*, 2015, **32**, pp. 1941–1946

[15] Huang L., Chowdhury D.R., Ramani S., *ET AL.*: 'Experimental demonstration of terahertz metamaterial absorbers with a broad and flat high absorption band', *Opt. Lett.*, 2012, **37**, pp. 154–156

[16] Pham V.T., Park J.W., Vu D.L., *ET AL.*: 'THz-metamaterial absorbers', *Adv. Nat. Sci. Nanosci. Nanotechnol.*, 2013, **4**, p. 015001

[17] Ye Y., Jin Y., He S.: 'Omnidirectional, polarization-insensitive and broadband thin absorber in the terahertz regime', *J. Opt. Soc. Am.*, 2010, **27**, pp. 498–504

[18] Ke Sh., Wang B., Huang H., *ET AL.*: 'Plasmonic absorption enhancement in periodic cross-shaped graphene arrays', *Opt. Express*, 2015, **23**, pp. 8888–8900

[19] Lin X., Wang Z., Gao F., *ET AL.*: 'Atomically thin nonreciprocal optical isolation', *Sci. Reports*, 2014, **4**, p. 4190

[20] Koppens F.H.L., Chang D.E., García de Abajo F.J.: 'Graphene plasmonics: a platform for strong light-matter interactions', *Nano Lett..*, 2011, **11**, pp. 3370–3377

[21] Sreekanth K.V., Zeng Sh., Shang J., *ET AL.*: 'Excitation of surface electromagnetic waves in a graphene-based bragg grating', *Sci. Rep.*, 2012, **2**, p. 737

[22] Gao W., Shu J., Qiu C., *ET AL.*: 'Excitation of plasmonic waves in graphene by guided-mode resonances', *ACS Nano*, 2012, **6**, pp. 7806–7813

[23] Barzegar-Parizi S., Rejaei B., Khavasi A.: 'Analytical circuit model for periodic arrays of graphene disks', *IEEE J. Quantum Electron..*, 2015, **51**, (9), pp. 1–7

[24] Khavasi A., Rejae B.: 'Analytical modeling of graphene ribbons as optical circuit elements', *IEEE J. Quantum Electron..*, 2014, **50**, (6), pp. 397–403